Structural, Magnetic, and Electrical Behavior of Low Dimensional Ba_2CoO_4

K. Boulahya,[†] M. Parras,[†] J. M. González-Calbet,*[,†] U. Amador,[‡] J. L. Martínez,[§] and M. T. Fernández-Díaz[||]

Departamento de Química Inorgánica, Facultad de Químicas, Universidad Complutense, E-28040 Madrid, Spain, Departamento de Química, Universidad San Pablo−CEU, E-28668 Madrid, Spain, Instituto de Ciencia de Materiales de Madrid, CSIC, Cantoblanco, E-28049 Madrid, Spain, and Institut Laue Langevin, BP 156X, F-38042 Grenoble, France

Received May 5, 2006. Revised Manuscript Received June 14, 2006

The cobaltite Ba_2CoO_4 presents a monoclinic symmetry (space group $P2_1/n$) and lattice parameters $a = 5.891\,31(7)$, $b = 7.59\,74(3)$, $c = 10.3638(2)$ Å, and $\beta = 91.90(1)°$. As determined from X-ray and neutron diffraction data, its structure can be described as formed by isolated CoO_4 tetrahedra defining zigzag rows running along the *a* axis, separated by Ba atoms in both the *b* and the *c* directions. The cobalt atoms are in a high spin Co^{4+} ground state, and their magnetic structure evidences the existence of antiferromagnetic and ferromagnetic alignments of the magnetic moments alternating along each of the aforementioned rows. Transport properties are related to p-type carriers.

Introduction

Magnetic, electrical, and catalytic properties of cobaltites make them promising materials for different applications. For instance, besides the interesting electrical properties of the system $La_{1-x}Sr_xCoO_{3-y}$,[1] giant magnetoresistance has been found in $La_{1-x}(Ba,Sr,Ca)_xCoO_{3-y}$[2] whereas thermoelectric power properties have been reported for $Ca_3Co_4O_9$.[3] The richness of the physical properties of the cobaltites is related to the ability of Co ions to adopt not only several oxidation states but also various spin states. This is well-known in the case of the $LaCoO_3$ perovskite where Co^{3+} exhibits spin state transitions as a function of the temperature.[4] In this three-dimensional structure, the $[CoO_6]$ octahedra share corners. When lanthanum is totally substituted by barium, the 2H-hexagonal perovskite $BaCoO_3$ is obtained, which, structurally, is a one-dimensional compound formed by a hexagonal array of chains of face-sharing $[CoO_6]$ octahedra.[5] In this phase, Co^{4+} is in the low spin configuration. The material is a semiconductor, and the reason for its poor conductivity has been suggested as due to Anderson localization.[6]

The introduction of anionic vacancies in $BaCoO_3$ breaks the polyhedral sequence of the 2H structure through the incorporation of $[BaO_2]$ cubic layers. Co is partially reduced to Co^{3+}, and besides in octahedral sites, it is also stabilized in a tetrahedral environment. In particular, we have recently reported the structural characterization and the physical properties of the $Ba_5Co_5O_{14}$ ($BaCoO_{2.80}$) phase.[7] $Ba_5Co_5O_{14}$ is structurally a two-dimensional compound in which Co_3O_{12} blocks, formed by three $[CoO_6]$ face-sharing octahedra, are linked through their terminal corners to two CoO_4 tetrahedra which define layers parallel to the basal plane (001). This material shows ferromagnetic behavior, and from an electrical point of view, it behaves as a low dimensional system with an Anderson localization state of the charge carriers.

Cobalt deficiency can be also introduced in the 2H framework, and it is accommodated by the introduction of Ba_3CoO_6 layers in the structure leading to the stabilization of cobalt in the trigonal prismatic environment. Depending on the Ba:Co ratio, a series of new materials, structurally one-dimensional, have been stabilized. They are constituted by a hexagonal array of isolated chains built from the ordered alternation of $[CoO_6]$ octahedra and trigonal prisms sharing faces. Depending on the ratio and the relative arrangement of both types of polyhedra a large number of phases have been stabilized.[8,9] Up to now the oxidation state of cobalt is unclear in these phases which, usually, show one-dimensional magnetic behavior.

As in 2H-$BaCoO_3$, cobalt is only present as Co^{4+} in Ba_2CoO_4, but their structures are strongly different. Actually, Ba_2CoO_4, isostructural to Ba_2TiO_4,[11] a distorted form of the

* To whom correspondence should be addressed. E-mail: jgcalbet@quim.ucm.es. Fax: (34) 91 394 43 52.
[†] Universidad Complutense.
[‡] Universidad San Pablo−CEU.
[§] CSIC.
[||] Institut Laue Langevin.

(1) Petrov, A. N.; Kononchuk, O. F.; Andreev, A. V.; Cherepanov, V. A.; Kofstad, P. *Solid State Ionics* **1995**, *80* (3−4), 189.
(2) Briceno, G.; Xiang, X. D.; Change, H.; Sun, X.; Schultz, P. G. *Science* **1995**, *270*, 273.
(3) Masset, A. C.; Michel, C.; Maignan, A.; Hervieu, M.; Toulemonde, O.; Studer, F.; Raveau, B.; Hejtmanek, J. *Phys. Rev. B.* **2000**, *62*, 166.
(4) Señaris-Rodríguez, M. A.; Goodenough, J. B. *J. Solid State Chem.* **1995**, *118*, 323.
(5) Hardy, A. *Acta Crystallogr.* **1962**, *15*, 179.
(6) Felser, C.; Yamaura, K.; Cava, R. J. *J. Solid State Chem.* **1999**, *146*, 411.
(7) Boulahya, K.; Parras, M.; González-Calbet, J. M.; Amador, U.; Martínez, J. L.; Fernández-Díaz, M. T. *Phys. Rev. B* **2005**, *71*, 144402.
(8) Boulahya, K.; Parras, M.; González-Calbet, J. M. *J. Solid State Chem.* **1999**, *142*, 419.
(9) Boulahya, K.; Parras, M.; González-Calbet, J. M. *Chem. Mater.* **2000**, *12*, 25.
(10) Boulahya, K.; Parras, M.; González-Calbet, J. M.; Vegas, A. *Solid State Science* **2000**, *2*, 57.
(11) Bland, J. A. *Acta Crystallogr.* **1961**, *14*, 875.

10.1021/cm061044v CCC: $33.50
Published on Web 07/14/2006

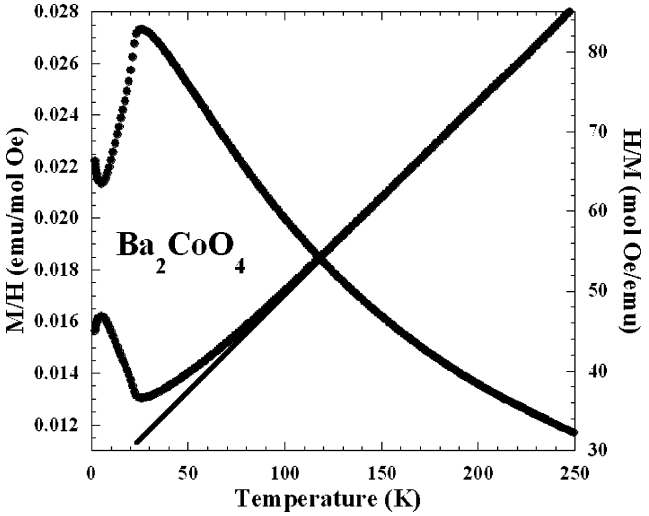

Figure 1. Dependence on temperature of the magnetic susceptibility (*M*/*H*) and inverse susceptibility (*H*/*M*) for Ba_2CO_4 for zero magnetic field cooling.

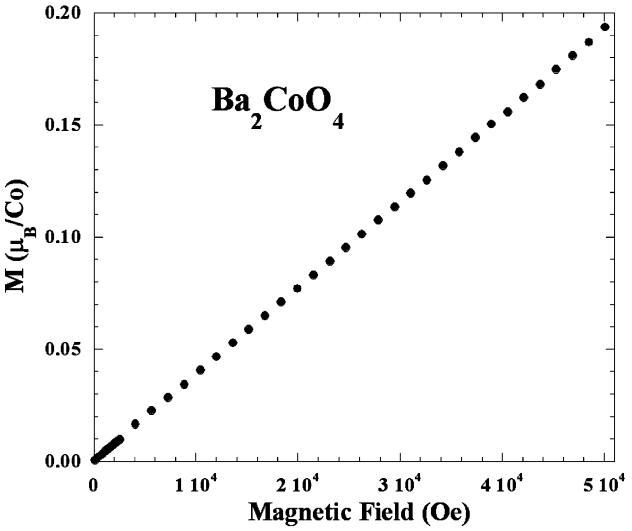

Figure 2. Magnetization dependence of the magnetic field at 5 K for Ba_2CoO_4.

orthorhombic K_2SO_4 structure type, shows cobalt ions only in the tetrahedral environment whereas they are octahedrally coordinated in the 2H structure. Co^{4+} also confers remarkable properties to another (214) material recently studied: Sr_2CoO_4. This oxide, isostructural to the K_2NiF_4 type with corner-sharing CoO_6 octahedra, exhibits a ferromagnetic transition with a rather high Curie temperature as well as metallic behavior[12] and large negative magnetoresistance.[13] It must be pointed out that there are few materials with all cobalt atoms in the Co^{4+} state at a tetrahedral site. One of the few reported oxides (together with Li_4CoO_4)[14] is Ba_2CoO_4. In both cases, despite such a particular feature, its physical properties have not been widely studied. This work involves the determination of both the nuclear and the magnetic structures of Ba_2CoO_4 using neutron diffraction at different temperatures, as well as the study of its magnetic and electrical properties.

Experimental Section

Polycrystalline Ba_2CoO_4 was synthesized by heating stoichiometric amounts of $BaCO_3$ (Aldrich, 99.98%) and Co_3O_4 (Aldrich, 99+%) in air at 900 °C for 3 days and then quenching to room temperature.

The average cationic composition was determined by inductive coupling plasma whereas the local composition was analyzed by energy-dispersive X-ray spectroscopy with an INCA analyzer system attached to a JEOL 3000 FEG electron microscope.

Powder X-ray diffraction (XRD) patterns were collected using Cu Kα radiation ($\lambda = 1.5418$ Å) at room temperature on a PHILIPS X'PERT diffractometer equipped with a graphite monochromator. Neutron powder diffraction (NPD) data were collected at room temperature and at 4 K on the diffractometer D1A at the Institute Laue Langevin (ILL), Grenoble (France), with neutrons of wavelength 1.908 Å; the angular range covered by the detector expands from 6 to 150° in scattering angle (step size 0.05°). Diffraction data were analyzed by the Rietveld method[15] using the Fullprof program.[16]

To follow the evolution of the ordered magnetic moment with temperature, a series of neutron diffraction patterns was recorded on the D1B powder diffractometer at the ILL, using neutrons of wavelength 2.52 Å, in the angular range from 10 to 90° (step size 0.2°). The temperature was changed sequentially from 4 to 60 K.

Magnetic properties were measured in a SQUID magnetometer, in a temperature range from 2 to 300 K and magnetic fields up to 5 T. Resistivity measurements were performed in a standard cryostat by the four-probe technique. Thermoelectric Seebeck coefficient experiments were performed on the PPMS cryostat from QD, San Diego. The specific heat was measured by the heat pulse relaxation method on the same PPMS system, at different external magnetic fields (up to 9 T) in a temperature range from 2 to 300 K. A ceramic pellet of the sample was placed on a sapphire platform with a small amount of Apiezon N grease, as the thermal contact. The signal coming from the addenda and the platform was measured in a separate run and subtracted from the experimental data.

Results

Physical Properties. The magnetic susceptibility (χ) for Ba_2CoO_4, measured using a magnetic field of 0.1 T, and its inverse ($1/\chi$) as a function of temperature are presented in Figure 1. The main feature is a clear peak in the magnetic susceptibility around 23 K, characteristic of antiferromagnetic interactions in the system. The data analysis of the inverse susceptibility with a Curie−Weiss law in the linear portion of the curve indicates a paramagnetic moment of 5.86 μ_B/Co ion and a Weiss constant $\Theta = -116$ K (in the range from 100 to 300 K). The calculated paramagnetic moment for Co^{4+} in a tetrahedral environment ($S = 5/2$) is 5.9 μ_B/Co, in agreement with the observed value. The inverse of the susceptibility deviates from a linear Curie Weiss behavior for temperatures below 100 K, still much higher than the observed $T_N = 23$ K. Such deviation could be due to the formation of correlated regions (clusters), due to a possible magnetic frustration resulting from the competition

(12) Matsuno, J.; Okimoto, Y.; Fang, Z.; Yu, X. Z.; Matsui, Y.; Nagaosa, N.; Kawasaki, M.; Tokura, Y. *Phys. Rev. Lett.* **2004**, *93*, 167202.
(13) Wang, X. L.; Takayama-Muromachi, E. *Phys. Rev. B* **2005**, *72*, 064401.
(14) Jansen, M.; Hoppe, R. *Naturwissenschaften* **1973**, *60*, 104.
(15) Rietveld, H. V. J. *Appl. Crystallogr.* **1969**, *2*, 65.
(16) Rodríguez-Carvajal, J. *Physica B* **1993**, *192*, 55.

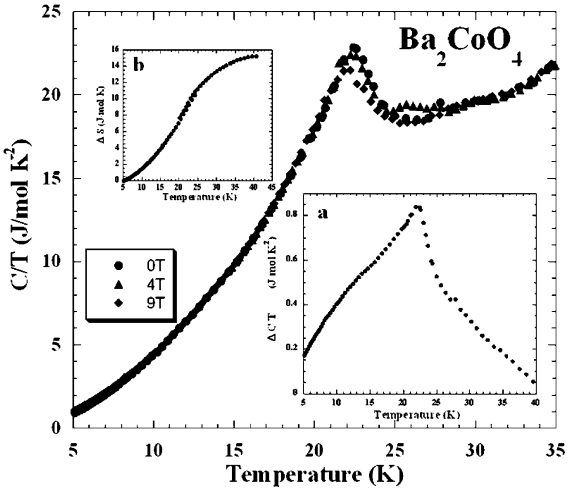

Figure 3. Temperature dependence of the magnetic specific heat for Ba_2CoO_4 at different applied external magnetic fields up to 9 T. Inset a shows C/T vs temperature at zero magnetic field for Ba_2CoO_4 with a clear phase transition at $T_N \approx 23$ K. Temperature dependence of the magnetic entropy for Ba_2CoO_4 is presented as inset b.

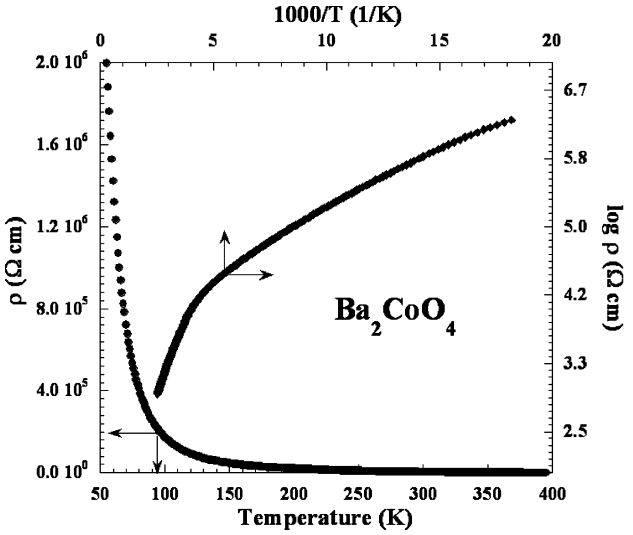

Figure 4. Temperature dependence of the resistivity for Ba_2CoO_4. The log ρ versus $1000/T$ is also included.

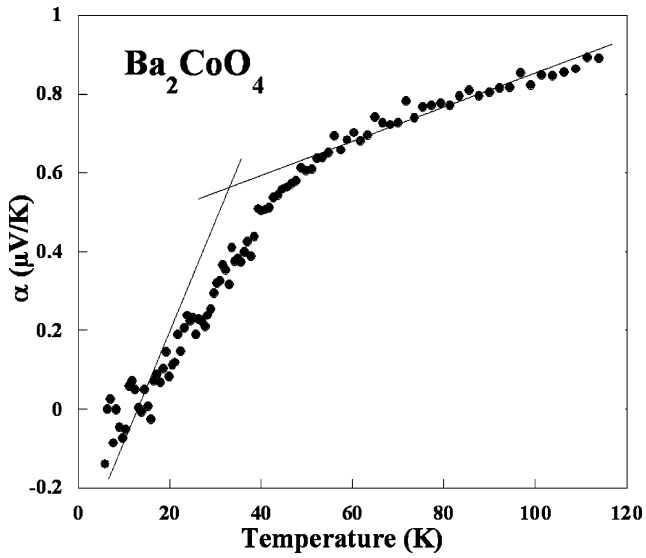

Figure 5. Dependence of the thermoelectric Seebeck coefficient on temperature for Ba_2CoO_4.

of several magnetic interactions present in the system (see below) and the hopping behavior shown in the electrical resistivity. The magnetic field dependence of the magnetization is presented in Figure 2, at 5 K for Ba_2CoO_4. A clear linear behavior is observed as expected for an antiferromagnetic ordered system.

The temperature dependence of the specific heat at different applied magnetic fields is depicted in Figure 3. A clear peak indicating a phase transition is observed at $T_N = 23$ K. As expected for an antiferromagnetic phase transition, the effect of a moderate external magnetic field is very weak. To evaluate the magnetic specific heat, we have to subtract the total specific heat from the phononic component (the electronic one is negligible because of the insulating character below 50 K). To calculate the contribution from phonons in this temperature range (below 30 K), a Debye model with T^3 dependence has been applied. The corrected magnetic specific heat is shown as inset a in Figure 3, with the antiferromagnetic phase transition producing a peak at 23 K. From these data, it is possible to calculate the magnetic entropy associated with the magnetic phase transition observed at 23 K. The magnetic entropy is depicted in inset b in Figure 3. The magnetic entropy associated with the transition is $\Delta S = 15$ J/mol K; the expected magnetic entropy related to Co^{4+} ($S = 5/2$) is 14.9 J/mol K, because calculated and experimental values are in very close agreement.

Electrical properties have also been investigated. The temperature dependence of the resistivity for Ba_2CoO_4 is presented in Figure 4. A clear semiconducting behavior is observed, with a resistivity out of the measuring range below 50 K. The data analysis starts with a typical activated conduction mechanism (T^{-1}); as observed in Figure 4, this model is only valid at high temperature (higher than 200 K). Different power laws were tested for a variable range hopping mechanism, from -1 to $-1/4$, all of them showing a linear behavior in the total temperature range. However, the standard Mott ($T^{-1/4}$) law fits much better than the T^{-1} one. The reason for that nonlinear behavior could be related to the structural anisotropy of the compound with strong one-dimensional character. A similar behavior is observed for doped $BaCoO_3$.[17] The shape of the resistivity plots does not provide enough evidence to determine a unique or dominant transport mechanism in this compound.

The temperature dependence of the thermoelectric Seebeck coefficient is shown in Figure 5. The application of an external magnetic field (up to 9 T) does not produce any observed variation of the Seebeck coefficient. This coefficient is weak and positive, indicating that dominant transport is related to p-type carriers (hole type). The Seebeck coefficient shows a clear change in the slope, around 23 K, that is, close to T_N approaching to zero when the temperature decreases. The above-mentioned conducting properties might be due to a certain degree of hybridization of the metal states with the oxygen band, as indicated also by the magnetic properties.

Structural Characterization. The average and local compositions determined on several dozens of small crystallites are in agreement with the nominal one. The oxygen

(17) Yamaura, K.; Cava, R. J. *Solid State Commun.* **2000**, *115*, 305.

Table 1. Structural Parameters Corresponding to the Nuclear and Magnetic Structures of Ba_2CoO_4 at 4 K[a]

atom	*x*/*a*	*y*/*b*	*z*/*c*	*B* (Å^2)
Ba(1)	0.2343(9)	0.4926(7)	0.1907(5)	0.7(1)
Ba(2)	0.757(1)	0.8521(6)	0.0833(6)	0.7(1)
Co	0.766(1)	0.277(1)	0.073(1)	1.3(2)
O(1)	0.516(1)	0.2045(8)	0.1666(5)	1.5(6)
O(2)	0.998(1)	0.1749(7)	0.1424(5)	1.5(6)
O(3)	0.7032(9)	0.186(8)	0.9185(6)	1.5(6)
O(4)	0.7740(9)	0.5072(7)	0.0806(5)	1.5(6)

Magnetic Structure[b] at 4 K

		moment (μ_B)	
atom	position	m_x	m_y
Co(1)	(0.383(1), 0.277(1), 0.036(1))[c]	−3.08(6)	0.9(1)
Co(2)	(0.367(1), 0.777(1), 0.213(1))[c]	3.08(6)	0.9(1)
Co(3)	(0.117(1), 0.723(1), 0.463(1))[c]	3.08(6)	−0.9(1)
Co(4)	(0.133(1), 0.223(1), 0.286(1))[c]	−3.08(6)	−0.9(1)

[a] Space group $P2_1/n$ (No. 14), $a = 5.891\,31(7)$ Å, $b = 7.5974(3)$ Å, $c = 10.3638(2)$ Å, $\beta = 91.90(1)°$, $V = 463.60(2)$ Å^3, $R_B = 0.059$, $R_{exp} = 0.049$, $R_{wp} = 0.072$, $\chi^2 = 1.62$. [b] $a_{mag} = 2a$, $b_{mag} = b$, $c_{mag} = 2c$; $R_{mag} = 0.083$. [c] Atoms originated from this by −1, +($^1/_2$ 0 0), and +(0 0 $^1/_2$) are AF coupled.

content, as determined by thermogravimetric analysis, is in agreement with the Ba_2CoO_4 composition.

The XRD pattern can be indexed on the basis of a monoclinic unit cell with lattice parameters $a = 5.8913(7)$ Å, $b = 7.5973(3)$ Å, $c = 10.3637(3)$Å, and $\beta = 91.93(1)°$, with no impurity phases being detected.

The refinement of the crystal structure was performed from a high-resolution NPD pattern collected at 4 K with 1.908 Å. The pattern was fitted with the $P2_1/n$ monoclinic space group starting with the model previously proposed from XRD data.[10] The obtained atom positions are the same within deviation errors, but we were able to determine more accurately the oxygen positions due to the characteristics of the neutron scattering. The measured *Q* range allows all the atomic coordinates as well as the isotropic Debye−Waller factors to be refined independently. The refinement of independent temperature factors is also possible, but because of the limited *Q* range, the obtained deviations are rather big. As the obtained values are quite similar for atoms belonging to the same chemical species, the isotropic temperature parameters were constrained to be equal for the same type of atom.

The main structural feature is the presence of isolated CoO_4 tetrahedra defining zigzag rows running along the *a* axis and separated by Ba atoms in both the *b* and the *c* directions. Two of these rows stacked along the *c* axis are displaced by $^1/_2a$. The average Co−O distances (1.776(9) Å) are rather short as expected for that high valence cation in tetrahedral coordination. They are similar to those found for Co^{4+} in tetrahedral coordination in comparable barium−cobalt oxides such as 12H-$BaCoO_{2.61}$[18] and 5H-$BaCoO_{2.80}$[7] or in Li_4CoO_4.[14] Table 1 collects some selected structural information of the material at 4 K. No vacancies were observed in the cationic substructure or in the anionic one. Accordingly, the chemical composition seems to be very close to the nominal one, Ba_2CoO_4, and, therefore, the cobalt oxidation state can be assumed to be four.

(18) Jacobson, A. J.; Hutchinson, J. L. *J. Solid State Chem.* **1980**, *35*, 334.

Table 2. Selected Interatomic Distances (Å) Less than 3.5 Å in Ba_2CoO_4 at 4 K

Ba(1)−O(1)	2.764(5)	Ba(2)−O(1)	3.035(6)	
Ba(1)−O(1)	2.665(5)	Ba(2)−O(1)	3.085(5)	
Ba(1)−O(2)	2.686(5)	Ba(2)−O(1)	3.0165(8)	
Ba(1)−O(2)	2.822(5)	Ba(2)−O(2)	2.796(5)	
Ba(1)−O(3)	2.722(4)	Ba(2)−O(2)	2.889(5)	
Ba(1)−O(3)	2.734(5)	Ba(2)−O(3)	2.728(5)	
Ba(1)−O(4)	2.810(5)	Ba(2)−O(3)	3.069(6)	
Ba(1)−O(4)	2.909(5)	Ba(2)−O(3)	3.192(5)	
Ba(1)−O(4)	3.416(6)	Ba(2)−O(4)	2.622(5)	
average	2.836(5)	average	2.937(6)	
Co−O(1)	1.872(9)			ordering
Co−O(2)	1.710(9)	Co(1)−Co(2)	5.29(2) × 2	AF
Co−O(3)	1.771(9)	Co(1)−Co(3)(1−1−1)[b]	5.28(1)	AF
Co−O(4)	1.752(9)	Co(1)−Co(3)(10−1)[b]	4.65(1)	AF
average	1.776(9)	Co(1)−Co(3)(0−1−1)[b]	5.43(1)	F
distortion[a]	4.48×10^{-3}	Co(1)−Co(3)(0 0−1)[b]	4.82(1)	F

[a] Distortion $= 1/n\{\sum[(d_i - \langle d\rangle)/\langle d\rangle]^2\}$. [b] Corresponding translation.

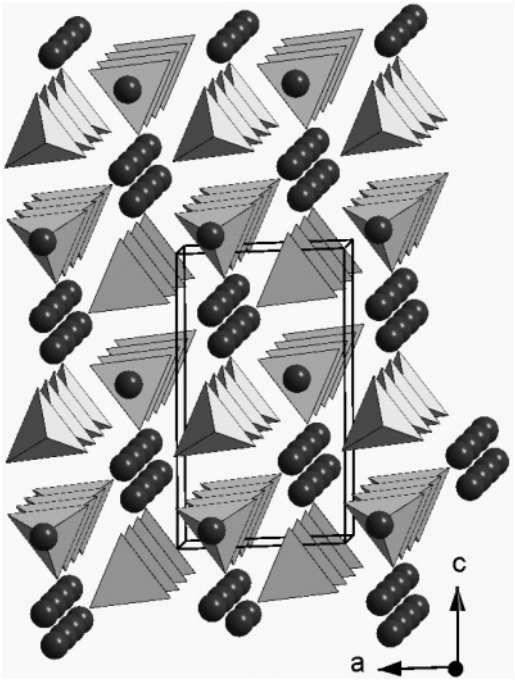

Figure 6. Schematic representation of the Ba_2CoO_4 nuclear structure. Black sphere, Ba; gray tetrahedra, CoO_4.

As shown in Table 2, each cobalt ion is surrounded by six other cobalt ions, the metal-to-metal distances ranging from 4.65 to 5.43 Å. Among them, the shortest Co−Co distances ($d_{Co-Co} = 4.65$ and 4.82 Å) are those previously defined within the mentioned CoO_4 tetrahedra rows running along the *a* axis, giving rise to a structure with a rather one-dimensional character. This structure has been represented in Figure 6 and is essentially maintained from room temperature to 4 K, because no structural transition is observed.

As discussed in relation to the structural and physical properties, the magnetic susceptibility measurements show an antiferromagnetic transition at a Neél temperature of $T_N = 23$ K. The NPD patterns of Ba_2CoO_4 obtained below the Neél temperature show the presence of low-angle additional peaks of magnetic origin. As the temperature decreases, the intensity of the magnetic peaks increases until nearly achieving saturation. These magnetic reflections can be indexed by using the propagation vector $\mathbf{k} = (0.5, 0, 0.5)$,

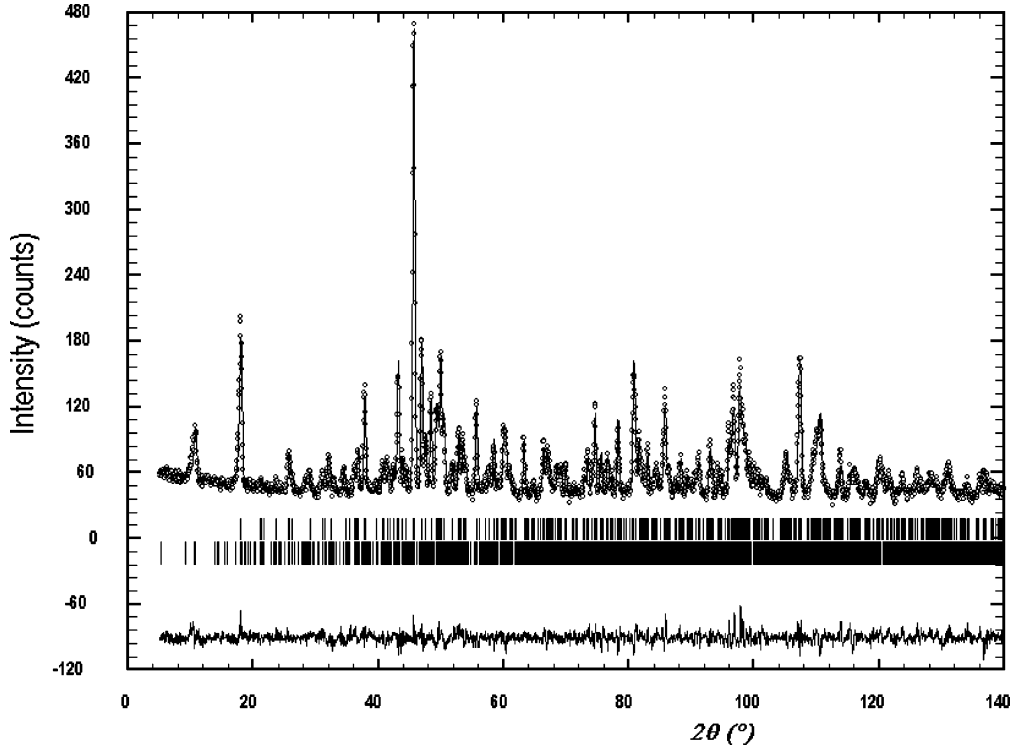

Figure 7. Graphic result of the fitting of the NPD data of Ba_2CoO_4 at 4 K: experimental (points), calculated (solid line), and difference (bottom).

Table 3. Irreducible Representations and Basis Functions of the Space Group $P2_1/n$ for the Wickoff Position 4e and Propagation Vector k = (0.5, 0, 0.5)[a]

irreducible representation		basis function vectors			
		Co(1)	Co(2)	Co(3)	Co(4)
$\Gamma_1(+\,+\,+\,+)$	$A_xC_yA_z$	(1 0 0)	(−1 0 0)	(−1 0 0)	(1 0 0)
		(0 1 0)	(0 1 0)	(0 −1 0)	(0 −1 0)
		(0 0 1)	(0 0 −1)	(0 0 −1)	(0 0 1)
$\Gamma_2(+\,+\,-\,-)$	$G_xF_yG_z$	(1 0 0)	(−1 0 0)	(1 0 0)	(−1 0 0)
		(0 1 0)	(0 1 0)	(0 1 0)	(0 1 0)
		(0 0 1)	(0 0 −1)	(0 0 1)	(0 0 −1)
$\Gamma_3(+\,-\,+\,-)$	$C_xA_yC_z$	(1 0 0)	(1 0 0)	(−1 0 0)	(−1 0 0)
		(0 1 0)	(0 −1 0)	(0 −1 0)	(0 1 0)
		(0 0 1)	(0 0 1)	(0 0 −1)	(0 0 −1)
$\Gamma_4(+\,+\,+\,+)$	$F_xG_yF_z$	(1 0 0)	(1 0 0)	(1 0 0)	(1 0 0)
		(0 1 0)	(0 −1 0)	(0 1 0)	(0 −1 0)
		(0 0 1)	(0 0 1)	(0 0 1)	(0 0 1)

[a] The characters (+ for 1, − for −1) of each symmetry operator are given in parentheses. The list corresponds to the following ordering of the symmetry operators, in Seitz notation: {1|000}, {2_0*y*0|*ppp*}, {-1|000}, {*m*_*x*0*z*|*ppp*}, with $p = 1/2$.

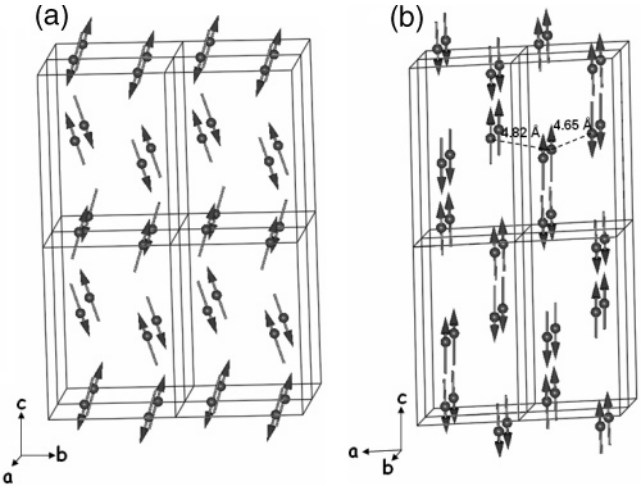

Figure 8. Magnetic structure of Ba_2CoO_4 at 4 K: (a) along the *a* axis and (b) along the *b* axis. The orientations of refined moments on Co sites are shown as arrows.

so the magnetic cell is doubled along the *a* and *c* axes with respect to the crystallographic cell.

To determine the magnetic structure, symmetry analysis for the space group $P2_1/n$ with the propagation vector $\mathbf{k} = (0.5, 0, 0.5)$ has been performed for the 4e position, occupied by the Co atoms in tetrahedral coordination. The output of the analysis is the complete set of basis functions of the irreducible representations classifying the possible magnetic ordering models, which is summarized in Table 3. Four one-dimensional real representations have been obtained. The notation for the atomic positions of the Co atoms are: Co(1) (x, y, z), Co(2) $(-x + 1/2, y + 1/2, -z + 1/2)$, Co(3) $(-x, -y, -z)$, and Co(4) $(x + 1/2, -y + 1/2, z + 1/2)$.

After checking all of the possible magnetic modes obtained, the best agreement with the experimental data was obtained for the magnetic structure given by the basis vectors of the irreducible representation Γ_1. This means that the magnetic moments become ordered with a spin arrangement given by $A_xC_yA_z$. The A_x basis vector implies that the coupling among the magnetic moments is $m_{1x} - m_{2x} - m_{3x} + m_{4x}$ (similarly for A_z), and the C_y basis vector implies that the *y* components are related by $m_{1y} + m_{2y} - m_{3y} - m_{4y}$.

The good agreement between the observed and calculated NPD patterns at $T = 4$ K is presented in Figure 7. As it is indicated in Table 1, at $T = 4$ K the total refined magnetic moment for the ordered cobalt atoms is $m = 3.23(6)\ \mu_B$. The resulting magnetic structure is a noncollinear antiferromagnetic ordering with the largest component of the magnetic moments lying along *c* direction with $3.08(6)\ \mu_B$, but the refinements give a small canting to the *b* direction of $0.9(1)\ \mu_B$. The magnetic structure of Ba_2CoO_4 determined

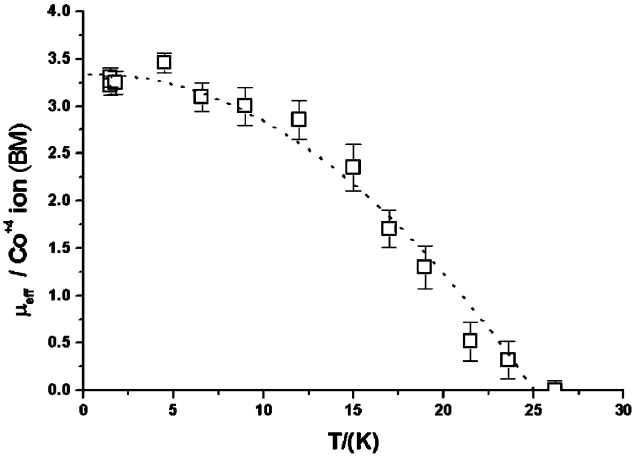

Figure 9. Temperature dependence of the ordered Co magnetic moment as obtained from the NPD data for Ba_2CoO_4.

from the neutron diffraction data has been represented in Figure 8 where two different orientations of the structure are shown.

Neutron diffraction patterns recorded at different temperatures have been used to follow the evolution of the intensities of the magnetic peaks so that the evolution of the ordered magnetic moment per cobalt ion as a function of temperature can be monitored. As a result of the low Q range of the D1B diffractometer, the crystal structure was kept fixed to that obtained at 4 K. The corresponding plot is shown in Figure 9. It is clearly observed that the magnetic moment decreased to zero level around 25 K, providing an estimation for the Néel temperature (T_N), in good agreement with that observed in the dependence on temperature of the magnetic susceptibility.

The obsevation of the obtained magnetic structure shows that several magnetic interactions have to be considered in this system. The first neighbor interaction seems to be a direct exchange between Co^{4+} cations, but as the shorter Co−Co distances are 4.65 and 4.82 Å, the direct overlap of the unpaired electron wave functions should be rather weak. The second kind of magnetic interactions should be of super-superexchange type where two neighboring Co atoms interact through two oxygen atoms; that is, the exchange pathway is of the type Co−O−O−Co. Such a type of interaction takes place for the next-nearest neighbors with distances of 5.28, 5.29, and 5.43 Å. The magnetic structure is the result of the competing magnetic interactions, and it presents antiferromagnetic alignment of the magnetic moments of the two cobalt ions separated by 4.65 Å, whereas ferromagnetic alignments exist between neighboring cobalt ions separated by 4.82 Å: alternating parallel and antiparallel orientations of the magnetic moments along a row. These rows are stacked parallel to each other in the b direction and give rise to rows of parallel cobalt moments along this direction.

Concerning the spin state of Co ions, the refinement of the magnetic structure for Ba_2CoO_4 revealed a reduction in the observed magnetic moment (3.23(6) μ_B) in comparison with the expected value of 5.9 μ_B. The formal Co^{4+} is a high valence state. In this case, the ground state of the material is dominated by the ligand−hole character, and the hybridization effects are important. The reduction of the ordered magnetic moment compared with the pure ionic configuration can be due to a combination of these covalence effects and zero-point fluctuation of the magnetic moments in AF structures.

Concluding Remarks

The nuclear and magnetic structures of Ba_2CoO_4 have been determined. The oxygen content corresponds to the nominal stoichiometry. As a consequence, all the Co ions are in the Co^{4+} electronic state, and they are tetrahedrally coordinated with four oxygen ions. The compound becomes magnetically ordered at $T_N = 23$ K as shown in the temperature dependence of both magnetic susceptibility and specific heat. The magnetic structure corresponds to a noncollinear antiferromagnetic mode with the magnetic moments oriented mostly along z and with a smaller y component. The Seebeck coefficient is positive, and the electrical behavior is characteristic of p-type carriers.

Acknowledgment. Financial support through research Project Nos. MAT2004-01248 and MAT/0627/2004 is acknowledged. K.B. thanks the MEC (Spain) for financial support under the "Ramón y Cajal" program. The authors thank the Institut Laue Langevin, Grenoble, France, for making availables its facilities.

CM061044V